DESIGN OF OPTIMIZED FIXED-POINT WCDMA RECEIVER

Hai-Nam Nguyen, Daniel Menard, and Olivier Sentieys

IRISA/INRIA, University of Rennes,
6 rue de Kerampont
F-22300 Lannion
Email: hanguyen@irisa.fr

ABSTRACT

To satisfy energy and complexity constraints, embedded wireless systems require fixed-point arithmetic implementation. To optimize the fixed-point specification, existing approaches are based on fixed-point simulations to evaluate the performances. In this paper the approach used to optimize the fixed-point specification is presented for the case of a WCDMA receiver. In our approach an analytical approach is used to evaluate the dynamic range and the fixed-point accuracy. Moreover for the bit error rate (BER), the analytical expression of the accuracy constraint according to the BER is proposed. The results show that the optimized fixed-point specification depends on the input receiver Signal-to-Noise ratio.

1. INTRODUCTION

Wireless communication domain is one of the most important sectors for Digital Signal Processing (DSP) applications [12]. The design of low cost and low power terminals is one of the key challenges in this domain. New services are provided (image, video, Internet access) and require high data rate. Consequently, the complexity of the baseband digital part is growing. Different aspects have to be considered to optimize the implementation cost and the power consumption. Especially, the arithmetic aspects offer opportunities to reduce the cost and the power consumption.

Efficient implementation of embedded wireless systems requires the use of fixed-point arithmetic. Therefore, the vast majority of embedded DSP applications is implemented in fixed-point architectures [1, 2, 11]. Indeed, fixed-point architectures are cheaper and more energy efficient than floating-point architectures because their data word-lengths are lower.

The fixed-point conversion process is made-up of two main steps corresponding to the dynamic range estimation and the fixed-point data word-length optimization. The aim of this optimization process is to minimize the implementation cost as long as the application performances are fullfiled. To optimize the fixed-point specification, existing approaches [13, 3] are based on fixed-point simulations to evaluate the performances. In [10], the fixed-point error is analyzed for a CDMA receiver, but the performances in terms of BER is also measured with fixed-point simulations. To evaluate accurately the BER, a great number of samples are needed. Each modification of the fixed-point data requires a new fixed-point simulation. Thus these approaches suffer from a major drawback which is the long optimization time. Consequently, the fixed-point design space can not be explored and multiple word-length approaches [4] can not be used.

In this paper the approach used to optimize the fixed-point specification is presented for the case of a WCDMA receiver. This technology is used for the physical layer of the third generation of wireless communication systems (UMTS). A new approach is proposed to estimate more accurately the data dynamic range. The properties of the application are taken into account to reduce the pessimistic effects of classical analytical approaches like interval arithmetic. Then, the accuracy constraint used in the fixed-point optimization problem is determined from the required application performances. For the bit error rate (BER), the analytical expression of the accuracy constraint according to the BER is proposed. The experiment results show the opportunity to code the fixed-point data according to the receiver Signal-to-Noise Ratio (SNR). Our approach can be easily adapted to any communication system.

The paper is organized as follows. In Section 2 the fixed-point conversion process is summarized and the WCDMA receiver is described in Section 3. The design of the symbol decoder module is detailed in Section 4. First, the dynamic range estimation is presented an secondly, the fixed-point specification optimization is described. In Section 5, the design of the searcher module is presented.

2. FIXED-POINT CONVERSION

The fixed-point conversion can be divided into two main modules corresponding to binary-point position determination and word-length optimization.The first part corresponds to the determination of the integer part word-length of each datum. The number of bits iwl_i for this integer part must allow the representation of all the values taken by the data, and is obtained from the data bound values. Thus, firstly the dynamic range is evaluated for each datum. Then, these results are used to determine, for each data, the binary-point position which minimizes the integer part word-length and which avoids overflow. Moreover, scaling operations are inserted in the application to adapt the fixed-point format of a datum to its dynamic range or to align the binary-point of the addition inputs.

The second part corresponds to the determination of the fractional part word-length. The number of bits fwl_i for this fractional part defines the computational accuracy. Thus, the data word-lengths are optimized. The output quantization noise power P_e is the metric used to evaluate the fixed-point computation accuracy. The implementation cost is minimized under the accuracy constraint $P_e^{\max}$. Let $\mathbf{wl}$ be an N-size vector including the word-length of the N application data. Let $C(\mathbf{wl})$ be the implementation cost and $P_e(\mathbf{wl})$ be the computational accuracy obtained for the word-length vector $\mathbf{wl}$. The implementation cost $C(\mathbf{wl})$ is minimized under the accuracy constraint $P_e^{\max}$:

$$\min\left(C\left(\mathbf{wl}\right)\right) \qquad \text{such as} \qquad P_e(\mathbf{wl}) \geq P_e^{\max} \tag{1}$$

To obtain reasonable optimization times, an analytical approach is used to evaluate the fixed-point accuracy. Moreover, a link between the application performances and the accuracy constraint must be done. An analytical expression of the maximal quantization noise power according to the performances is proposed for the BER at the rake receiver output.

3. PRESENTATION OF WCDMA

WCDMA is a standard for the third-generation of cellular network which is based on DS-CDMA (Direct Spread Code Division Multiple Access) technology. In WCDMA, two layers of spreading codes are used [5]: channelization code and scrambling code. The channelization code C_{ch} is used to achieve orthogonality between channels when time-shift is equal to zero. The scrambling codes used in uplink are Gold codes C_G. The input data d_t is multiplied with the spreading codes, and the transmitted signal Tx_t is equal to $\mathrm{Tx}_t = d_t C_{ch} C_G$. In a multi-path Rayleigh channel, the global

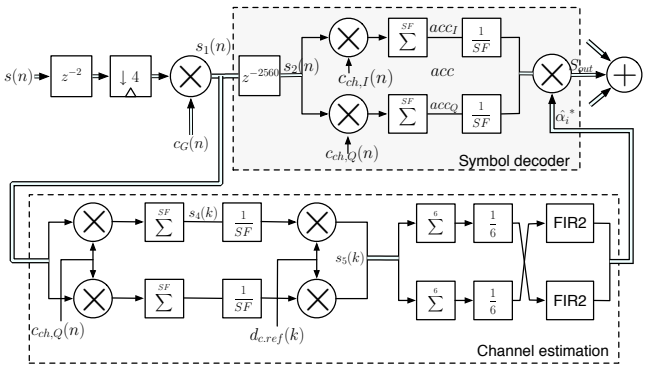

Figure 1: Data flow graph of the i^{th} finger of the WCDMA rake receiver.

received signal $s(n)$ is the sum of elementary signal $s^i_{in}(n)$ for different channel paths. Let τ_i and α_i be respectively the delay and the complex amplitude of i^{th} path in the channel. The global received signal $s(n)$ expression is equal to

$$s(n) = \sum_i s^i_{in}(n) + n_{in}(n) = \sum_i \alpha_i \mathrm{Tx}(n-\tau_i) + n_{in}(n) \qquad (2)$$

The term $n_{in}(n)$ represents the noise term and is made-up of the receiver thermal noise and the interference of the other users. This term can be considered gaussian with variance $\sigma^2_{n_{in}}$. Assuming that a user has one DPDCH channel, $d_t C_{ch}$ take values in $\{\pm 1 \pm i\}$. Thus $\mathrm{Tx} \in \{\pm 2, \pm 2i\}$. For simplification, Tx is normalized into $\{\pm 1, \pm i\}$, hence its power is equal to one. By definition, the Signal-to-Noise Ratio (SNR) is equal to :

$$SNR = \frac{2E_b}{N_0} = \frac{1}{\sigma^2_{n_{in}}} \qquad (3)$$

For the WCDMA receiver, the symbol decoding is carried-out by a rake receiver to benefit from the effects of multi-path fading. The concept of the rake receiver is based on the combination of the different multi-path components in order to improve the quality of the decision on the symbol. Each multi-path signal is processed by a finger which correlates the received signal by a spreading code aligned with the delay τ_i of the multi-path signal. The multi-path components can be considered as uncorrelated when the delay exceeds a chip period. Demodulation results of a weighted decision at the correlator outputs. Using the maximum likelihood criteria the symbol is estimated from the $y(k)$ signal

$$y(k) = \sum_{i=1}^{N_p} y_i(k) = \sum_{i=1}^{N_p} \alpha^*_i(k) r_i(k) \qquad (4)$$

Thus, the finger is made-up of two main parts corresponding to the decoding symbol module and the channel estimation module. The data flow graph of symbol decoder module is presented in Figure 1. The complex amplitude α_i of the i^{th} path is estimated with the help of the known pilot sequence located in the control frame (DPCCH). Thanks to the complex multiplication of the received signal by the conjugate of the Kasami code the unscrambling operation is performed. Then, the despreading operation from OVSF code transforms the wide band received signal into a narrow band signal. Finally, the estimated phase distortion resulting of the transmission channel is removed.

Each finger requires the knowledge of the delay τ_i of the i^{th} path to obtain the maximal correlation. First, the coarse time delay estimation is carried-out with the path searcher. Then, the fine synchronization of the code and the received signal is made with a Delay-Locked Loop (DLL). The data flow graph of the path searcher is presented in Figure 2.

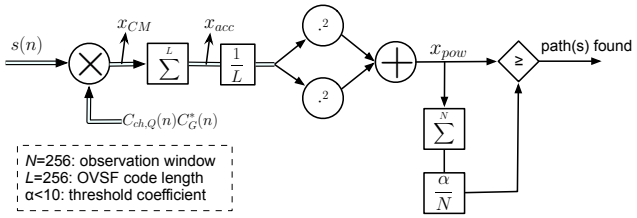

Figure 2: Data flow graph of the path searcher.

4. SYMBOL DECODER

4.1 Dynamic range estimation

The first step of the fixed-point conversion process corresponds to the determination of the data integer word-length. This step requires to determine each data dynamic range. An analytical approach based on interval arithmetic [6] is used to estimate the dynamic and to guarantee no overflow. However, this method sometimes overestimates the dynamic range if the application properties are not taken into account.

In a direct sequence spead-spectrum system, the Signal-to-Noise Ratio is particularly low. With tens of simultaneous users in communications, the noise and interference power is tens of times higher than the useful signal. The dynamic range is mainly due to the noise and interference. In the de-spreading process, the signal is summed up over the length L of spreading sequence. The pure analytical approach will multiply the dynamic range by L. But this process multiplies mainly the dynamic range of useful signal, not that of noise and interference. From this property, an approach is then proposed to determine more accurately the data dynamic range. Before the de-spreading/correlation process, the whole useful signal plus noise is considered. After this process, only the useful signal is taken into account when calculating the dynamic range.

The dynamic range of the different data is computed from the rake-receiver flow graph presented in Figure 1. The input $s(n)$ consisting of desired signal $s^i_{in}(n)$ plus noise $n_{in}(n)$ is normalized to have the maximum amplitude of both real and imaginary parts one. Because a gaussian noise $\sigma^2_{n_{in}}$ has 99.7% of its values in the interval $[-3\sigma_{n_{in}}, 3\sigma_{n_{in}}]$, assuming the real and imaginary parts of $s^i_{in}(n)$ are in the interval $[-1,1]$, the input is considered in the interval $[-1-3\sigma_{n_{in}}, 1+3\sigma_{n_{in}}]$. The normalization process corresponds to the division of the input by $1+3\sigma_{n_{in}}$.

By propagating the input range in the flow graph, the following results are obtained. The dynamic range of the accumulator output acc_I before normalization is equal to

$$\max(|acc_I|) = \frac{4.SF}{1+3\sigma_{n_{in}}} \qquad (5)$$

The dynamic range of α_i corresponding to the output of the channel estimation module is equal to

$$\max(|\alpha_i|) = \frac{1}{1+3\sigma_{n_{in}}} \qquad (6)$$

The dynamic range of s_{out} corresponding to the output of the channel estimation module is equal to

$$\max(|s_{out}|) = \frac{4}{(1+3\sigma_{n_{in}})^2} \qquad (7)$$

The dynamic range has been estimated with our analytical approach for different SNR values and compared with results obtained from simulations. The results are presented in Figure 3 for the accumulator output (acc_I) and for the symbol decoding output (s_{out}). It is noticed that from one to two bits differ between estimated and simulated results. Nevertheless, the evolutions of the dynamic range according to the SNR are identical for analytical and simulation

based estimations. This confirms the validity of our approach to estimate the dynamic range in the WCDMA receiver. The difference between the two lines can be explained by the channel model used in the simulation. If a single path channel model, for example, is used, the difference is less than 1 bit. Moreover, the analytical estimations are known to be more pessimistic. In both simulation and estimation, for the accumulation output, there is a difference of 3 bits between 0 dB and 25 dB. For the finger output, there is a difference of 4 bits between 0 dB and 15 dB and of 6 bits between 0 dB and 25 dB. These results show the opportunity to adapt the integer part of the data according to the SNR at the receiver input.

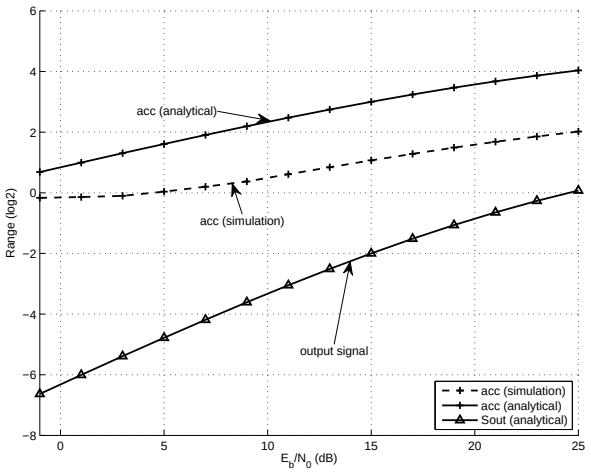

Figure 3: Estimated and simulation based values of dynamic range for the decoder.

4.2 Word-length optimization

In fixed-point implementation, a minimal computation accuracy must be provided to guarantee that the system performances are maintained. For the symbol decoding module as well as the whole system, the performances are evaluated with the bit-error rate (BER) so that the use of finite precision does not modify the reference infinite precision BER (BER_0) more than ε. Suppose that the power of quantization noise e_q is P_e, the performance criterion can be written as:

$$\mathrm{BER}_0 \leq P_e \leq (1+\varepsilon)\mathrm{BER}_0 \tag{8}$$

4.2.1 Accuracy constraint

Noise Model

The quantization noise can be modeled by a sum of different noise sources propagating throughout the system. This sum can be considered as a single noise source $\widetilde{e_q}$ at the system output. In [8], this noise source $\widetilde{e_q}$ is validated for a wide range of applications as the sum of a uniform-distributed noise and a gaussian noise:

$$\widetilde{e_q} = \upsilon(\beta \times e_u + (1-\beta) \times e_n) \tag{9}$$

where e_u and e_n are uniform-distributed noise and gaussian noise with variance of 1, υ controls the variance (power) of the global noise and $\beta \in [0,1]$ is a weight allowing the combination of two models. If there is a dominant quantization noise source, the output noise is fairly a uniform distribution and $\beta \approx 1$. In the other extremity, where each noise source contributes the same, $\beta \approx 0$. This model is valid for every systems based on arithmetic operations and using rounding quantization mode.

Constraint determination

In this part, the expression of the bit error rate $\mathrm{BER}(P_e)$ according to the output quantization noise power P_e is presented. This expression allows determining the maximum quantization noise power satisfying (8). First the case of a gaussian distribution for the output quantization noise is considered ($\beta = 0$). Inside the system, multiple rounding quantization noises $e_1, e_2, ..., e_K$ are generated. If there is no dominant noise source, due to the central limit theorem, the sum of these noises is then considered gaussian and has the following probability density function (pdf):

$$f_q(x) = \frac{1}{\sigma_q\sqrt{2\pi}} \exp \frac{-x^2}{2\sigma_q^2} \tag{10}$$

where

$$\sigma_q^2 = \sum_{i=1}^{K} \sigma_{e_i}^2 \tag{11}$$

In a WCDMA receiver, the thermal noise and multiple-access interference can be modeled as a gaussian noise source if the transmission channel is AWGN and there is no dominant interferers [9]. In other cases, improved gaussian approximation or alternative method must be used. For simplicity, at first, the received signal is assumed to have two components corresponding to the desired signal and the gaussian noise and interference. Thus, the output is the sum of the output quantization noise e_q and the output receiver noise n_{out}. The expression of the total noise probability density function $f_n(x)$ is as follows:

$$f_n(x) = \frac{1}{\sqrt{\sigma_{n_{out}}^2 + \sigma_q^2}\sqrt{2\pi}} \exp \frac{-x^2}{2(\sigma_{n_{out}}^2 + \sigma_q^2)} \tag{12}$$

and the following probability distribution function $F_n(x)$:

$$F_n(x) = \frac{1}{2}\left(1 + \mathrm{erf}\,\frac{x}{\sqrt{\sigma_{n_{out}}^2 + \sigma_q^2}\sqrt{2}}\right) \tag{13}$$

Since WCDMA uses BPSK/bi-orthogonal transmission, bit-error rate can be calculated as follow:

$$\begin{aligned}\mathrm{BER}(\sigma_q, \sigma_{n_{out}}) &= 1 - F_n(1) = \frac{1}{2}\,\mathrm{erfc}\,\frac{1}{\sqrt{\sigma_{n_{out}}^2 + \sigma_q^2}\sqrt{2}} \\ &= Q\left(\frac{1}{\sqrt{\sigma_{n_{out}}^2 + \sigma_q^2}}\right)\end{aligned} \tag{14}$$

From (8) and (14), the condition for σ_q^2 is:

$$\begin{aligned}\sigma_q^2 &\leq \frac{1}{2}\mathrm{erfc}^{-1}\left((1+\varepsilon)\,\mathrm{erfc}\,\frac{1}{\sigma_{n_{out}}\sqrt{2}}\right)^{-2} - \sigma_{n_{out}}^2 \\ &= Q^{-1}\left((1+\varepsilon)Q\left(\frac{1}{\sigma_{n_{out}}}\right)\right)^{-2} - \sigma_{n_{out}}^2\end{aligned} \tag{15}$$

Secondly, the case with a dominant quantization noise has been considered ($\beta = 1$). In this case, the noise distribution is uniform and its probability density function $f_q(x)$ is then as follows:

$$f_q(x) = \frac{1}{q}\mathbf{Id}_{[\frac{-q}{2}, \frac{q}{2}]} \tag{16}$$

Thus the global noise has the following probability density function:

$$f_n(x) = f_c * f_q(x) = \int_{-\infty}^{\infty} f_c(t) f_q(x-t)\,dt \tag{17}$$

$$= \frac{1}{2q}\left(\mathrm{erf}\,\frac{x + \frac{q}{2}}{\sqrt{N_0}} - \mathrm{erf}\,\frac{x - \frac{q}{2}}{\sqrt{N_0}}\right) \tag{18}$$

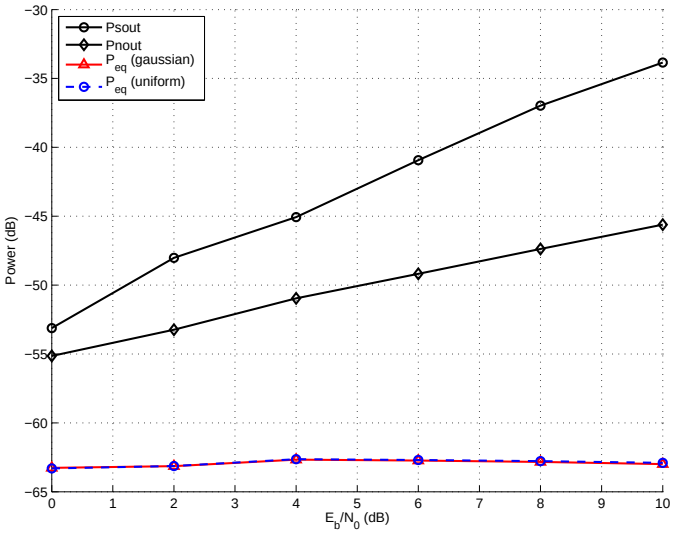

Figure 4: Signal and noise power levels according to the SNR

and the following probability distribution function:

$$F_n(x) = \int_{-\infty}^{x} \frac{1}{2q}(\text{erf}\frac{t+\frac{q}{2}}{\sqrt{N_0}} - \text{erf}\frac{t-\frac{q}{2}}{\sqrt{N_0}}) \quad (19)$$

In case of BPSK, the probability of bit error is:

$$\text{BER}(\sigma_q, \sigma_{n_{out}}) = 1 - F_n(1) \quad (20)$$

By the similar way, the precision can be deduced from Equation 8 and Equation 20. Since there is no simple mathematical expression, the criterion is solved numerically.

The accuracy constraint has been determined for different SNR values. The results are presented in Figure 4. The line $P_{s_{out}}$ and $P_{n_{out}}$ correspond to the level (power) respectively of the desired signal s_{out} (symbol) and the receiver noise n_{out} at the system output. The difference between the lines $P_{s_{out}}$ and $P_{n_{out}}$ corresponds to the output signal-to-noise ratio (SNR). The difference between the lines $P_{s_{out}}$ and P_{e_q} corresponds to the output signal-to-quantization noise ratio (SQNR).

The results show that to decrease the BER when the SNR increases, the SQNR must be increased. More accuracy is required to reduce the decision errors due to finite precision arithmetic.

4.2.2 *Computation accuracy evaluation*

To compute the power expression of the output quantization noise, the technique presented in [7] is used. Given that the code and the channel complex amplitude are constant for a frame, the system can be assumed to be linear and time invariant. For the choice of the code and the channel complex amplitude, the worst case which leads to the maximal quantization noise power is considered. The output quantization noise is a weighted sum of each noise source variance $\sigma^2_{q_i}$:

$$P_e = \sum_i K_i \sigma^2_{e_i} \quad (21)$$

with K_i, the gain between the output and the noise source. The variance $\sigma^2_{e_i}$ of each noise source is obtained from the quantization step q_i (LSB weight) obtained after quantization

$$\sigma^2_{e_i} = \frac{q^2}{12} \quad (22)$$

4.2.3 *Word-length optimization*

The optimization process presented in equation (1) is carried-out with the accuracy constraint defined in equation (15). The optimized word-lengths obtained for different SNR values are presented in Table 1. The results show that the optimized word-lengths vary according to the SNR. Between, 0 dB and 20 dB the word-length of the variables *acc* and s_{out} are increased of respectively 80 % and 66%. Optimization results show that, for a SNR varying from 0 dB to 20 dB, potentially, up to 40% of energy consumption can be saved if the fixed-point specification is adapted according to the SNR.

E_b/N_0 (dB)	1	3	5	7	9	11	13	15	17	19	21
acc	5	6	6	6	7	7	7	7	9	9	9
s_{out}	6	7	7	7	8	9	9	9	9	9	10

Table 1: Optimized word-lengths of the rake receiver obtained for different SNR values

5. PATH SEACHER

In this section the results obtained for the path searcher are presented.

5.1 Range estimation

The approach used for the rake-receiver to estimate the dynamic range is used for the path searcher described in Figure 2. The input data RX is normalized into $[-1,1]$. It is then multiplied with complex conjugate of spreading code $C_{ch}C^*_G$ and results in the interval $[-2,2]$ for each real and imaginary part. For the accumulation along with L symbols (L: OVSF code length) only the signal is summed up significantly. Thus, the dynamic range is equal to

$$\max(|x_{acc}|) = \frac{2L}{1+3\sigma} \quad (23)$$

The dynamic range of x_{pow} corresponding to the profile power is equal to

$$\max(|x_{pow}|) = \frac{8}{(1+3\sigma)^2} \quad (24)$$

The estimated and simulation based dynamic range of each value is presented in Figure 5. It is noteworthy that estimated and simulated results differ of 1 or 2 bits.

5.2 Precision evaluation

The path searcher module can not use criteria presented in 4.2. This module is based on the decision theory and classical criteria are used to analyze the performances. The *misdetections* (MD) corresponding to the non-detection of an existing path and the *false-alarms* (FA) corresponding to the detection of a non-existing path are measured.

To analyze the path searcher performances, the multi-path Rayleigh channel is considered. The output of the path searcher before decision x_{pow} is made-up of three components corresponding to the signal s_{pow}, the receiver noise n_{pow} and the output quantization noise e_q. Compared to the rake receiver, the distribution of the output signal is not straight. Two cases have to be considered. When there is a path, the output value depends on the module of the complex amplitude α_i associated to i^{th} path. Without path, the output values depend on the code properties. In this last case, the modelization of the output signal distribution is complex. Thus, the technique based on simulation presented in [8] has been retained to determine the accuracy constraint and a monte-carlo approach is used to measure the FA and MD values.

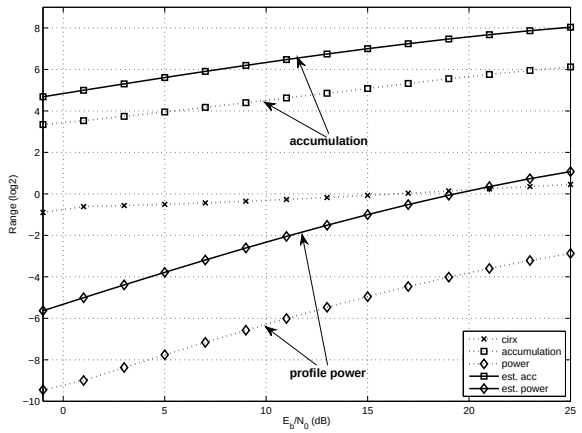

Figure 5: Estimated and simulation based values of range for the path searcher.

The evolution of the false-alarm according to the SNR are presented in Figure 6 for different levels of output quantization noise. The false-alarms are more sensitive than the mis-detections to the quantization noise. For the same level of quantization noise, the mean number of mis-detected paths does not evolve and is very closed to the case of infinite precision. Thus, the accuracy constraint is determined from the false alarm criteria and then the data word-lengths are optimized. The results are presented in Table 2. Like for the rake receiver, the word-lengths depend on the SNR values.

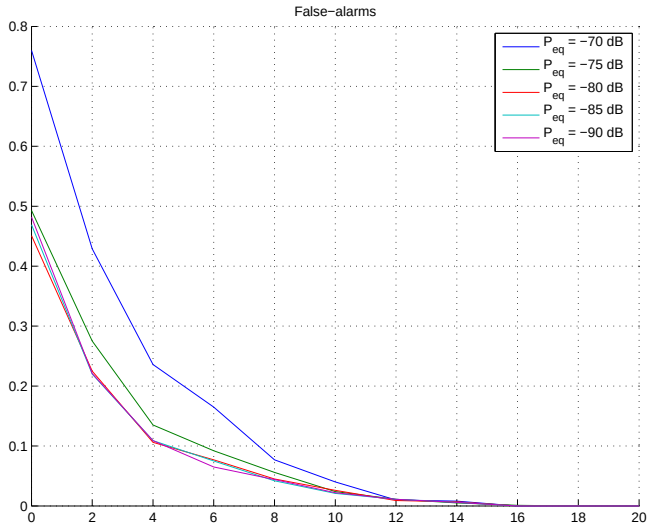

Figure 6: Mean number of non-valid detected paths (false alarm) obtained for different SNR values

6. CONCLUSION

For the design of embedded wireless systems, the optimization arithmetic aspects is one of the way to reduce the implementation cost and the power consumption. An approach has been proposed to optimize the fixed-point specification according to the required application performances. A new approach has been proposed to estimate more accurately the data dynamic range by exploiting the application properties. The accuracy constraint has been determined from the required application performances. For the bit error rate (BER), the analytical expression of the accuracy constraint according to the BER has been proposed. The results show that the fixed-point specification depends on the input SNR. An approach in which the fixed-point specification is adapted dynamically according to the input receiver SNR can be investigated. In the case of low SNR, lower word-length data can be used and energy can be saved.

E_b/N_0 (dB)	1	3	5	7	9	11	13	15	17	19	21
x_{CM}	8	8	8	8	8	8	8	8	9	9	9
x_{acc}	11	11	11	11	12	12	12	13	13	13	13
x_{pow}	7	6	7	7	8	9	9	10	10	11	11

Table 2: Optimized word-lengths of the searcher obtained for different SNR values

REFERENCES

[1] B. Evans. Modem Design, Implementation, and Testing Using NI's LabVIEW. In *National Instrument Academic Day*, Beirut, Lebanon, June 2005.

[2] J. Eyre and J. Bier. The evolution of DSP processors. *IEEE Signal Processing Magazine*, 17(2):43–51, March 2000.

[3] K. Han, I. Eo, K. Kim, and H. Cho. Numerical word-length optimization for CDMA demodulator. In *Circuits and Systems, 2001. ISCAS 2001. The 2001 IEEE International Symposium on*, volume 4, 2001.

[4] N. Herve, D. Menard, and O. Sentieys. Data wordlength optimization for FPGA synthesis. *Signal Processing Systems Design and Implementation, 2005. IEEE Workshop on*, pages 623–628, 2005.

[5] H. Holma and A. Toskala. *WCDMA for UMTS: Radio Access for Third Generation Mobile Communications*. Wiley, 2004.

[6] R. Kearfott. Interval Computations: Introduction, Uses, and Resources. *Euromath Bulletin*, 2(1):95–112, 1996.

[7] D. Menard, R. Rocher, and O. Sentieys. Analytical Fixed-Point Accuracy Evaluation in Linear Time-Invariant Systems. *IEEE Transactions on Circuits and Systems I: Regular Papers,*, 55(1), November 2008.

[8] D. Menard, R. Rocher, O. Sentieys, and O. Serizel. Accuracy Constraint Determination in Fixed-Point System Design. *EURASIP Journal on Embedded Systems*, Accepted for publication in 2008.

[9] M. Pursley. Performance Evaluation for Phase-Coded Spread-Spectrum Multiple-Access Communication–Part I: System Analysis. *Communications, IEEE Transactions on [legacy, pre-1988]*, 25(8):795–799, 1977.

[10] C. Sengupta, S. Das, J. R. Cavallaro, and B. Aazhang. Fixed point error analysis of multiuser detection and synchronization algorithms for cdma communication systems. In *in Proc. of ICASSP'98*, pages 3249–3252, 1998.

[11] W. Strauss. DSP chips take on many forms. DSP-FPGA.com Magazine, March 2006.

[12] W. Strauss. Hanging up on analog and flexing Wireless/DSP muscles. Technical report, Forward Concepts, 2008.

[13] H. Zhao, T. Ottosson, E. Strom, and A. Kidiyarova-Shevchenko. Performance analysis of a fixed-point successive interference canceller for wcdma. *Vehicular Technology Conference, 2004. VTC2004-Fall. 2004 IEEE 60th*, 3:1919–1923 Vol. 3, Sept. 2004.